May 2003

Magnetic hysteresis of mechanically alloyed Sm–Co nanocrystalline powders

J. Zhou
University of Nebraska - Lincoln

Ralph Skomski
University of Nebraska-Lincoln, rskomski2@unl.edu

David J. Sellmyer
University of Nebraska-Lincoln, dsellmyer@unl.edu

Magnetic hysteresis of mechanically alloyed Sm–Co nanocrystalline powders

J. Zhou,[a] R. Skomski, and D. J. Sellmyer
Behlen Laboratory of Physics and Center for Materials Research and Analysis, University of Nebraska, Lincoln, Nebraska 68588

(Presented on 12 November 2002)

Mechanically alloyed Sm–Co powders and $Sm_{12}(Co,Cu,Ti)_{88}$ powders are investigated. X-ray diffraction patterns show that after annealing, structures of 2:7, 1:5, and 1:7 phases form. A room-temperature coercivity of 41 kOe was obtained in Sm_2Co_7 powders. Magnetic hysteresis was investigated by the method of δm curves. Positive value δm curves were obtained in Sm_2Co_7 and $SmCo_5$, while negative values were found in $SmCo_{7.3}$ and $SmCo_8$ indicating different magnetization reversal mechanisms. Nanocrystalline powders of $Sm_{12}(Co,Cu,Ti)_{88}$ with a mixture of 1:5 and 2:17 phases form after long-time heat treatment. The intrinsic coercivity of the powders increases with an increasing amount of Cu. Short annealing time produces 1:7 phase with higher crystalline anisotropy, which results in larger coercivity. © *2003 American Institute of Physics.*
[DOI: 10.1063/1.1558587]

I. INTRODUCTION

Mechanical alloying (MA) and mechanical milling (MM) have been used extensively to obtain nanocrystalline and nanocomposite magnetic materials with significant improvement of magnetic properties.[1] In MA or MM Sm–Co permanent magnets, large coercivity and enhancement of remanence can be achieved through controlled grain size, fine microstructures, and large anisotropy field. Ding *et al.* reported a 57 kOe coercivity in a $Sm_{0.19}Co_{0.81}$ MA powder.[2] Sm_2Co_{17}:Co and $SmCo_5$:Fe MA nanocomposites were reported by Chen *et al.*[3] and Zhang *et al.*[4] Recently, Chen *et al.* reported the magnetic properties of mechanically milled $Sm_2(CoM)_{17}$, where M represents Zr, Hf, Nb, V, Ti, Cr, Cu, and Fe.[5] It is well known that two-phase Sm–Co 2:17-type magnets have a cellular microstructure, consisting of a 2:17 main phase surrounded by a Cu-rich 1:5 grain-boundary phase.[6] A similar nanostructure is realized in $Sm(Co,Cu,Ti)_z$ two-phase magnets.[7] In this article, we investigate mechanically alloyed $SmCo_z$ and $Sm(Co,Cu,Ti)_z$ magnets. Particular emphasis is on the magnetization reversal magnetism.

II. SAMPLE PREPARATION AND CHARACTERIZATION

Sm_2Co_7, $SmCo_5$, and Co powders are used to prepare Sm–Co MA powders. Sm, Co, Cu, Ti elemental powders are used to obtain Sm–Co–Cu–Ti powders. The starting materials are sealed in a vial together with hardened-steel balls under Ar atmosphere. The compositions studied are Sm_2Co_7, $SmCo_5$, $SmCo_{7.3}$, $SmCo_8$, and $Sm_{12}Co_{88-x-y}Cu_xTi_y$ with $x=0$, 4, 6, 7, 8, 9 and $y=0$, 3. Mechanical alloying is done by placing the vial in a high-energy Spex 8000 mixer/mill and milling for 5 h. Heat treatment is performed by sealing the powder in a quartz tube in an Ar atmosphere and then annealing in the range between 725 and 825 °C for 5 or 30 min. The crystal structure is examined by x-ray diffraction with Cu $K\alpha$ radiation. A superconducting quantum interference device magnetometer and a vibrating sample magnetometer with a high-temperature oven are used to measure the magnetic properties.

X-ray diffraction (XRD) patterns show the as-milled powder is in the ''x-ray'' amorphous state. Sm–Co powders are heat treated at 800 and 775 °C for 5 min. The XRD patterns show 2:7, 1:5, 1:7, and 1:7 phases corresponding to the powder compositions of Sm_2Co_7, $SmCo_5$, $SmCo_{7.3}$, and $SmCo_8$, respectively. $Sm_{12}(Co,Cu,Ti)_{88}$ powders show mainly the 2:17 structure after annealing at 825 °C for 5 or 30 min. Figure 1 shows the development of crystallization of $Sm_{12}Co_{81}Cu_4Ti_3$ powder for different annealing times. There is a small amount of the 1:5 phase present, also. There may be a small amount of 1:7 phase, but it cannot be determined due to the overlapping of peaks. Based on the calculation from Scherrer's formula, the average grain size ranges is about 35–50 nm and does not increase much with further annealing. XRD patterns for other Sm–Co–Cu–Ti compositions show similar results.

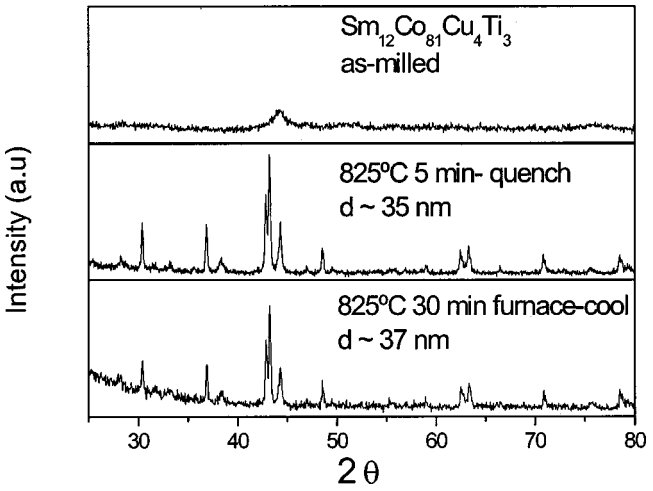

FIG. 1. X-ray diffraction patterns of mechanical alloyed $Sm_{12}Co_{81}Cu_4Ti_3$.

[a]Electronic mail: jzhou@unlserve.unl.edu

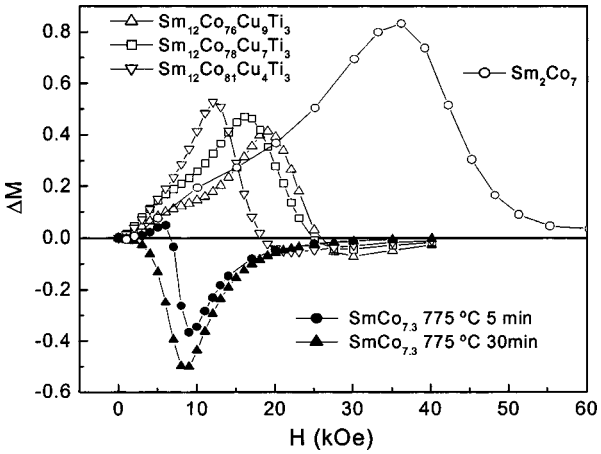

FIG. 2. Δm curves of Sm_2Co_7, $SmCo_{7.3}$, and Sm–Co–Cu–Ti.

III. MAGNETIC PROPERTIES

Magnetic hysteresis measurements at room temperature show single-phase behavior for all the samples. For Sm_2Co_7, $SmCo_5$, $SmCo_{7.3}$, and $SmCo_8$ alloy powders, the coercivities binary are 29, 8, 41, and 6 kOe, respectively. This is due to the smaller anisotropy constants in Co-rich alloys [$K_1 = 17.2\,\mathrm{MJ\,m^{-3}}$ for $SmCo_5$ and 3.3 $\mathrm{MJ\,m^{-3}}$ for Sm_2Co_{17} (Ref. 8)]. Δm curves of these samples are measured to investigate the magnetic hysteresis mechanism. Sm_2Co_7 and $SmCo_5$ samples show positive Δm value while $SmCo_{7.3}$ (shown in Fig. 2) and $SmCo_8$ show negative value. We also observed similar Δm curves in Sm–Co thin films.[9] The explanation for this difference will be discussed and compared to Sm–Co–Cu–Ti powders later.

Table I shows the magnetic properties of Sm–Co–Cu–Ti powders. It can be seen that for binary $Sm_{12}Co_{88}$, H_c is as low as 5.6 kOe. The remanence ratio (M_r/M_s) is close to 0.5, the ratio expected for randomly oriented uniaxial-anisotropy particles. The coercivity and remanence ratio are increased by the substitution of Ti or Cu for Co. In sintered Sm–Co 2:17-type magnets, Cu is introduced to form the precipitated Cu-rich grain boundary that provides pinning centers for domain-wall motion.[7,10] According to Chen *et al.*,[5] in powder form Cu helps the formation of 1:5 phase and Zr goes to 2:17 phase. 1:5 and 2:17 grains are uniformly distributed in the powder particles. Our samples containing Ti likely have similar structures. We know that Ti usually takes the Co dumbbell sites, which will increase the anisotropy of the SmCo alloys,[11] and Cu-rich phases, most likely 1:5, provide pinning centers to impede domain-wall motion, which increases the coercive force.

TABLE I. Magnetic properties of Sm–Co–Cu–Ti powders.

	825 °C, 30 min			825 °C, 5 min	
	H_c (kOe)	M_r (emu/g)	M_s (emu/g)	H_c at 27 °C	H_c at 400 °C
$Sm_{12}Co_{88}$	5.7	53	112		1.8
$Sm_{12}Co_{82}Cu_6$	9.7	50	101		2.0
$Sm_{12}Co_{85}Ti_3$	12.7	56	97		3.8
$Sm_{12}Co_{81}Cu_4Ti_3$	12.6	49	80	15.2	3.2
$Sm_{12}Co_{79}Cu_6Ti_3$	12.0	49	81		2.6
$Sm_{12}Co_{78}Cu_7Ti_3$	16.2	48	77	19.7	3.3
$Sm_{12}Co_{77}Cu_8Ti_3$	15.8	48	79	17.2	3.5
$Sm_{12}Co_{76}Cu_9Ti_3$	17.1	45	73	22.2	4.0

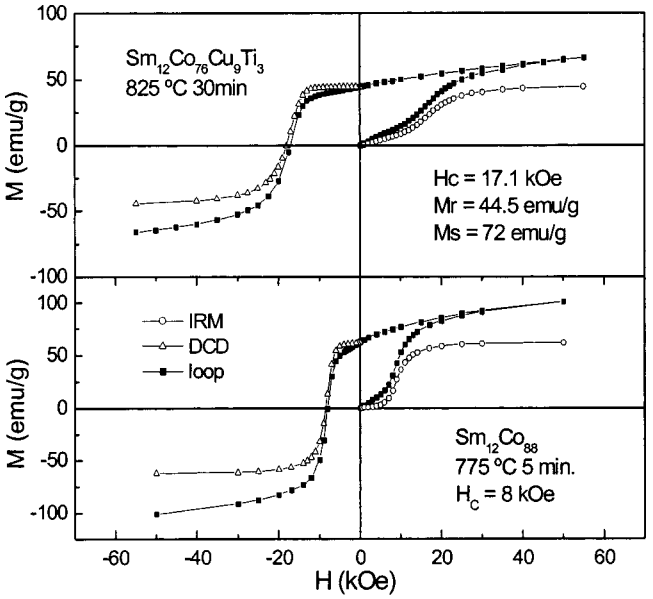

FIG. 3. Initial IRM, and DCD curves of $Sm_{12}Co_{88}$ and $Sm_{12}Co_{76}Cu_9Ti_3$.

All the samples heat treated at 825 °C for 5 min show larger H_c than those annealed for 30 min with the same compositions. This can be understood as a longer heat treatment produces larger crystallite size, as well as decomposes the 1:7 phase into 1:5 and 2:17 phases. The relatively low anisotropy of the 2:17 phase makes the coercivity of the powder smaller.

The high-temperature coercivity of the powder samples shows that H_c decreases as the temperature increases. This is mainly due to the change of anisotropy with the changing temperature. It can be seen that the high-temperature coercivity does not increase with additional Cu in $Sm_{12}Co_{85}Ti_3$. That is because Cu decreases both Curie temperature and the high-temperature anisotropy of the $SmCo_5$ phase.

IV. MAGNETIZATION REVERSAL MECHANISM

To understand the coercivity mechanism of the Sm–Co-based mechanical alloys we investigated the remanent-magnetization Δm behavior. Δm is defined as $\Delta m = m_d - (1-2m_r)$ where m_d is the reduced magnetization from DCD measurement and m_r is the reduced remanence from IRM measurement. According to Wohlfarth, the deviation is zero for non-interacting uniaxial single-domain particles.[12] It is commonly accepted that a negative δm value indicates the dipole interactions[13] and a positive value indicates ferromagnetic exchange interactions between isolated single-domain particles. Several papers discussed the magnetization behavior in permanent-magnet materials,[14,15] including the influence of the pinning mechanism on Δm. Skomski gave an example that domain-wall pinning also can generate a positive Δm.[16] Vajda *et al.* also pointed out that the demagnetization state will influence the Δm behavior.[17] Other researchers have explained the positive value of Δm as evidence of

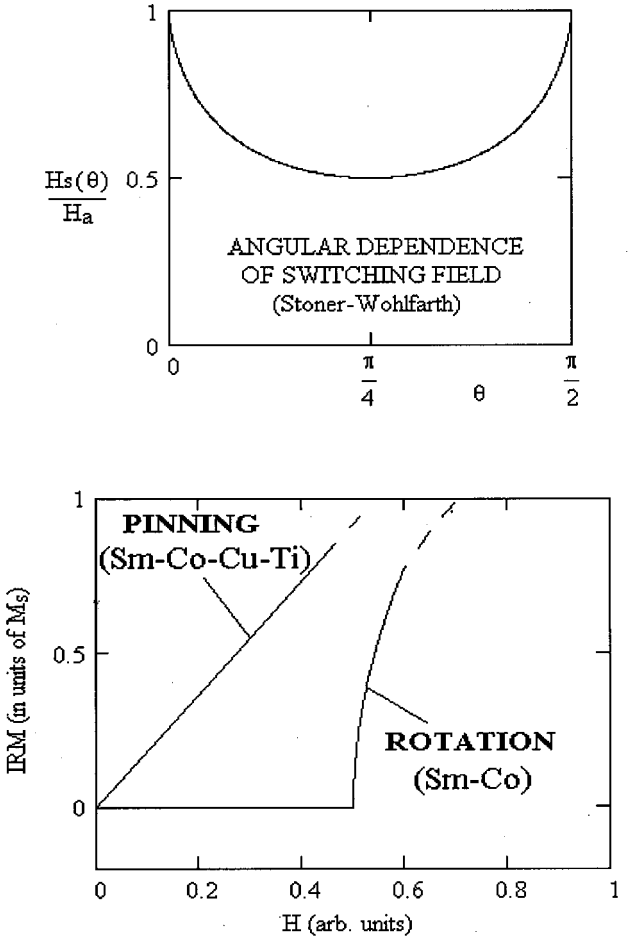

FIG. 4. Switching fields and IRM curves (schematic).

exchange interactions in nanocomposite between the hard and soft magnetic materials.[18,19] In this work, we attribute the Δm behavior to the basic mechanisms of coercivity: wall pinning or incoherent rotation.

In our experiment, the initial samples are in thermally demagnetized state. Figure 3 shows the initial curve, IRM and DCD curves for mechanically alloyed $Sm_{12}Co_{88}$ and $Sm_{12}Co_{76}Cu_9Ti_3$ powders. Other samples show similar behaviors. It can be seen that in Fig. 3(a), the remanence from the IRM curve gradually increases with the increasing field and the difference between IRM and initial curves is small before the field reaches the coercive field. This indicates that the magnetization process is mainly controlled by domain-wall pinning. During the process, the domain walls move overcoming the impedance from the pinning centers that are Cu- and Ti-containing phases. When the field is removed, the remanence is retained because the domain walls are pinned. The initial curve is also consistent with the typical curve for the Sm–Co 2:17 magnet with a distribution of pinning centers.[8] Sm_2Co_7 and $SmCo_5$ showing positive Δm value in Fig. 2 have similar IRM and DCD behaviors, but the coercivity is controlled by nucleation, not pinning. The strong exchange interactions tend to align the magnetization of grains. So during the magnetization process, when the field is removed, remanence is retained as a result of intergrain exchange interactions. Thus, a positive Δm curve is obtained.

In Fig. 3(b), for $Sm_{12}Co_{88}$ powders, the IRM remanence remains almost unchanged at low field, while the initial curve at the corresponding field gives a large magnetization. This is because of the coercivity mechanism in these powders is mainly incoherent rotation. According to Stoner and Wohlfarth's model,[8,20] the switching field H_s, at which the change in the equilibrium direction of magnetization becomes discontinuous, is given by[8]

$$H_s = \frac{2K_1}{\mu_0 M_s} \frac{1}{(\cos^{2/3}\Theta + \sin^{2/3}\Theta)^{3/2}}.$$

Figure 4(a) shows the angular dependence of the switching field in the model. Considering that the $Sm_{12}Co_{88}$ powder is an ensemble of weakly interacting fine particles with random orientation, ideally a small reverse field $H < 0.5 H_A$ (anisotropy field) yields a reversible rotation of the magnetization direction, but in large reverse fields the magnetization is irreversible.[8] Figure 4 shows the theoretical IRM curves for the two different magnetization reversal mechanisms.

Figure 3 shows the Δm curve of Sm–Co–Cu–Ti and Sm–Co powders. Because of the different IRM behaviors, Δm yields different values. In this case, negative Δm for Co-rich Sm–Co is due to the incoherent rotation and positive Δm for Sm–Co–Cu–Ti comes from the domain-wall pinning, while positive Δm for Sm_2Co_7 and $SmCo_5$ (not shown, similar to that of Sm–Co–Cu–Ti) is due to strong exchange interaction.

This work is supported by DOE, AFOSR, DARPA/ARO, and CMRA.

[1] P. G. McCormick, W. F. Miao, P. A. I. Smith, J. Ding, and R. Street, J. Appl. Phys. **83**, 6256 (1998), and references therein.
[2] J. Ding, P. G. McCormick, and R. Street, J. Alloys Compd. **191**, 197 (1993).
[3] S. K. Chen, J. L. Tsai, and T. S. Chin, J. Appl. Phys. **79**, 5964 (1996).
[4] J. Zhang, S. Y. Zhang, H. W. Zhang, and B. G. Shen, J. Appl. Phys. **89**, 5601 (2001).
[5] Z. Chen, X. Meng-Burany, H. Okumura, and G. C. Hadjipanayis, J. Appl. Phys. **87**, 3409 (2000).
[6] K. Kumar, J. Appl. Phys. **63**, R13 (1988).
[7] J. Zhou, R. Skomski, C. Chen, G. C. Hadjipanayis, and D. J. Sellmyer, Appl. Phys. Lett. **77**, 1514 (2000).
[8] R. Skomski and J. M. D. Coey, *Permanent Magnetism* (Institute of Physics, Bristol, 1999).
[9] D. J. Sellmyer, J. Zhou, Y. Liu, and R. Skomski, Proceedings of the 17th Work Shop on Rare-Earth Magnets and Their Applications, Delaware (2002).
[10] J. Zhou, R. Skomski, and D. J. Sellmyer, IEEE Trans. Magn. **37**, 2518 (2001).
[11] J. Zhou, I. A. Al-Omari, J. P. Liu, and D. J. Sellmyer, J. Appl. Phys. **87**, 5299 (2000).
[12] E. P. Wohlfarth, J. Appl. Phys. **29**, 595 (1954).
[13] J. Garcia-Otero, M. Porto, and J. Rivas, J. Appl. Phys. **87**, 7376 (2000).
[14] P. Gaunt, G. Hadjipanayis, and D. Ng, J. Magn. Magn. Mater. **54-57**, 841 (1986).
[15] F. E. Pinkerton and D. J. Van Wingerden, J. Appl. Phys. **60**, 3685 (1986).
[16] R. Skomski and D. J. Sellmyer, J. Appl. Phys. **89**, 7263 (2001).
[17] F. Vajda, E. Della Torre, and R. D. McMichael, J. Appl. Phys. **75**, 5689 (1994); R. D. McMichael, F. Vajda, and E. Della Torre, *ibid.* **75**, 5692 (1994).
[18] W. C. Chang, S. H. Wu, B. M. Ma, C. O. Bounds, and S. Y. Yao, J. Appl. Phys. **83**, 2147 (1998).
[19] Z. Chen, H. Okumura, G. C. Hadjipanayis, and Q. Chen, J. Appl. Phys. **89**, 2299 (2001).
[20] E. C. Stoner and E. P. Wohlfarth, Philos. Trans. R. Soc. London, Ser. A **240**, 599 (1948); IEEE Trans. Magn. **27**, 3475 (1991).